NASA Technical Memorandum 86977



# Oxidation and Hot Corrosion of Hot-Pressed $Si_3N_4$ at 1000 °C

William L. Fielder
*Lewis Research Center*
*Cleveland, Ohio*



April 1985

NASA

# OXIDATION AND HOT CORROSION OF HOT-PRESSED $Si_3N_4$ AT 1000 °C

William L. Fielder
National Aeronautics and Space Administration
Lewis Research Center
Cleveland, Ohio 44135



## SUMMARY

The oxidation and hot corrosion of a commercial, hot-pressed $Si_3N_4$ were investigated at 1000 °C under an atmosphere of flowing $O_2$. For the hot corrosion studies, thin films of $Na_2SO_4$ were airbrushed on the $Si_3N_4$ surface. The hot corrosion attack was monitored by the following techniques: continuous weight measurements; $SO_2$ evolution; film morphology; and chemical analyses.

Even though the hot corrosion weight changes after 25 hr were relatively small, the formation of $SiO_2$ from oxidation of $Si_3N_4$ was an order of magnitude greater in the presence of molten $Na_2SO_4$ than for oxidation in the absence of $Na_2SO4$. The formation of a protective $SiO_2$ phase at the $Si_3N_4$ surface is minimized by the fluxing action of the molten $Na_2SO_4$ thereby allowing the oxidation of the $Si_3N_4$ to proceed more rapidly. A simple process has been proposed to account for the hot corrosion process.

## INTRODUCTION

Efficiencies of heat engines are directly related to their operating temperatures. Today's high-temperature superalloys can be used up to about 1100 °C without cooling. To permit significant increases in operating temperatures, new classes of materials will be required. Ceramics is one class that shows promise. To date, only $Si_3N_4$ and SiC are being considered because they have certain desirable properties such as oxidation resistance, low thermal expansion characteristics, hardness, and strength retention (ref. 1).

Thermodynamically, $Si_3N_4$ is unstable to oxidation and is dependent upon the formation of a protective $SiO_2$ film for its existance. Several investigators have studied the kinetics and mechanisms of oxidation of hot-pressed $Si_3N_4$ (refs. 2 to 4).

In gas turbine engines, Na2SO4 deposition on superalloy turbine components can lead to severe corrosion by an accelerated oxidation process. This oxidation process in the presence of molten $Na_2SO_4$ is known as hot corrosion (ref. 5). In a similar manner, $Si_3N_4$ turbine components might also be susceptible to hot corrosion degradation. That is, the protective $SiO_2$ film might be fluxed by the molten $Na_2SO_4$ thereby exposing the unprotected $Si_3N_4$ surface to more rapid oxidation. Several attempts have been made to observe this type of attack on $Si_3N_4$ and SiC ceramics. For example, dynamic hot corrosion studies of $Si_3N_4$ have been made using burner rigs (refs. 6 and 7). Most of the hot corrosion laboratory tests have involved exposure to molten $Na_2SO_4$ (thick film exposure) in crucibles (ref. 8). A recent thin film study was concerned with the hot corrosion of sintered SiC (ref. 9).

The purpose of the present investigation is to observe the hot corrosion attack, using thin films of $Na_2SO_4$, of a high density $Si_3N_4$ in an oxidizing atmosphere. High density materials have been produced by a hot-pressing technique using dopants of MgO or $Y_2O_3$ (ref. 10). One commercially available, hot-pressed $Si_3N_4$ (produced by Norton Company as NCX-34) was of particular interest since it contained 2 to 3 percent W introduced by powder grinding with WC balls. Studies have shown that oxidation (in the absence of $Na_2SO_4$) may be increased by W (ref. 11).

The processes occurring during the hot corrosion of this NCX-34 $Si_3N_4$, which contained $Y_2O_3$ as the dopant and W as a major impurity, were investigated by the following techniques: by continuous monitoring of the weight changes by means of a sensitive electrobalance; by continuous monitoring of $SO_2$ evolution; by optical and electron microscopy; and by chemical analysis.

## EXPERIMENTAL

The $Si_3N_4$ starting material (NCX-34) was, primarily, β $Si_3N_4$ with 5.6 wt % Y, 3.1 W, 3.1 O and smaller quantities (0.1 to 0.2 percent) of Fe, Al, Na, and Pb. Since the $Si_3N_4$ contained $Y_2O_3$ as the dopant and WC as a major impurity, the molar composition was: 0.82 $Si_3N_4$, 0.10 $SiO_2$, 0.04 $Y_2O_3$, and 0.02 WC. This composition is close to the maximum for the compatibility triangle of $Si_3N_4$-$Si_2ON_2$-$Y_2Si_2O_7$ as seen in figure 1 (ref. 12). The density of the $Si_3N_4$ was about 3.30 g $cm^{-3}$ or about 98 percent theoretical of the starting material of the above composition.

Each sample was cut to about 1.8 cm by 0.5 cm by 0.25 cm using a diamond saw. A small hang-hole (0.15 cm o.d.) was drilled through the sample using a SiC sand blaster. The sample was smoothed using 600 grit SiC paper and then ultrasonically cleaned.

For oxidation studies, the cleaned samples were used without further treatment. For hot corrosion studies, the cleaned samples were heated on a hot plate and then coated with about 4.5 mg $cm^{-2}$ of $Na_2SO_4$ by airbrushing the surface with a saturated solution of $Na_2SO_4$. The sample was suspended inside a quartz tube from one arm of a sensitive electrobalance by means of a Pt wire. An atmosphere of $O_2$ was passed over the sample at a flow rate of about 8.3 $cm^3$ $sec^{-1}$ (a linear rate of 1.64 cm $sec^{-1}$). A Pt honeycomb catalyst was placed immediately downstream of the sample to equilibrate the evolved $SO_2$ with $O_2$ and $SO_3$. The furnace was then raised quickly to heat the sample to 1000 °C. Continuous weight and temperature measurements were recorded as voltages on a computer disk. The sample was quenched by lowering the furnace and the sample stored in a dessicator until needed.

Attempts to monitor the $SO_2$ evolution by means of a high pressure mass spectrometric sampling technique (ref. 13) were not successful. The $SO_2$ and $SO_3$ peak heights were small and erratic suggesting that the $SO_2$ and $SO_3$ concentrations probably were less than 5 ppm (the estimated limits for this technique).

Determining the $SO_2$ concentrations (simultaneously with weight measurements) was accomplished by means of a pulsed fluorescence $SO_2$ analyzer. The total S in the flowing $O_2$-$SO_2$ gas could be calculated from the $SO_2$-$SO_3$ equilibrium (i.e., $SO_3$ = 0.147 $SO_2$ for 1 atm of $O_2$).

The films (both surface and cross section), produced at the $Si_3N_4$ surface during hot corrosion at 1000 °C, were observed by metallography, SEM, and EDAX (energy dispersive x-ray) analyses. Cross sectioning of the samples were made by cutting the corroded samples carefully using a diamond saw and anhydrous kerosene as the coolant. For the SEM and EDAX observations, the surfaces were coated with Pd by sputtering.

Several samples, containing $Na_2SO_4$ coatings of about 4.5 mg $cm^{-2}$, were hot corroded at 1000 °C for times ranging from about 1 to 26 hr. The films, produced at the surface, were removed by the following sequential leeching treatments: (1) hot $H_2O$; (2) $HNO_3$; (3) acidic HF, and (4) neutralizing an aliquot of the acidic HF leech liquor with $NH_4OH$. Each liquor was analyzed for sulfate by an x-ray fluorescence technique (ref. 14). And, several of the liquors were analyzed for W and Y by atomic emission spectroscopy. An unreacted $Si_3N_4$ sample was treated similarly and used as a standard blank.

## RESULTS

The results obtained for the oxidation and hot corrosion of the hot-pressed $Si_3N_4$ starting material are given in the following six sections: (1) weight changes during oxidation; (2) weight changes during hot corrosion; (3) $SO_2$ evolution; (4) calculated $SiO_2$ formation during hot corrosion; (5) film morphology; and (6) chemical analyses.

### Weight Changes During Oxidation

A typical weight change curve is shown in figure 2 for the oxidation of $Si_3N_4$ (without a $Na_2SO_4$ coating) at 1000 °C. Beyond about 8 hr, the sample lost weight since losses from Pt chain evaporation now exceeded gains from oxidation of the sample. For observing $Si_3N_4$ oxidation, the usefulness of this curve is limited to less than about 8 hr due to the errors introduced by these evaporation losses. The smoothed data for the first 7.5 hr is replotted in figure 3. Since figure 3 suggests a parabolic-type relation, the smoothed data is replotted in figure 4 as the square of the specific weight gain with time. After correcting for evaporation losses, the calculated values (given by the circles) could be fitted, after 2 hr, to one straight line. A parabolic weight gain rate constant, R, of about $2 \times 10^{-12}$ $g^2$ $cm^{-4}$ $sec^{-1}$ was obtained.

### Weight Changes During Hot Corrosion

The results obtained during the hot corrosion at 1000 °C of a sample containing a $Na_2SO_4$ coating of 4.0 mg $cm^{-2}$ are plotted in figure 5. For comparison, weight changes obtained during the oxidation of $Si_3N_4$ without $Na_2SO_4$ are also shown as a dashed line. The results obtained for samples that were hot corroded for times greater than 35 hr are not shown. Beyond 35 hr, evaporation losses exceeded the oxidation weight gains. As seen in figure 5, the sample initially lost about 0.7 mg $cm^{-2}$ (2.1 mg) during hot corrosion. But, starting at about 12 hr, the sample gained weight and by about 30 hr had regained most of this initial weight loss. Evaporation losses are becoming increasingly important after 25 hr. In figure 6, the smoothed weight gain data (corrected for evaporation losses) are plotted as circles. This data could be fitted to

one straight line between about 28 and 35 hr. A parabolic weight gain rate constant, R', of about $1 \times 10^{-12}$ $g^2$ $cm^{-4}$ $sec^{-1}$ was obtained.

In figure 7, typical weight curves are given for hot corrosion of samples which contained $Na_2SO_4$ coatings at various levels. These curves suggest that the hot corrosion process, as indicated by the weight loss maximum and the time required to reach this maximum, is directly related to the quantity of $Na_2SO_4$ applied initially to the samples.

## $SO_2$ Evolution

Gaseous $SO_2$ is evolved during the $Na_2SO_4$ decomposition. In the presence of the Pt catalyst, the $SO_2$ produced should equilibrate with the $O_2$ atmosphere to produce a smaller quantity of $SO_3$. The $SO_2$ concentration in the flowing $O_2$ (after equilibration) is measured by the pulsed fluorescence $SO_2$ technique. A typical curve is given in figure 8. For this run, a sample (containing an initial coating of $Na_2SO_4$ of 4.5 mg $cm^{-2}$) was hot corroded at 1000 °C under 8.3 $cm^3$ $sec^{-1}$ of flowing $O_2$. Initially, the $SO_2$ concentration increased for a very short time (i.e., about 0.1 to 0.2 hr) and then it decreased to about 1 ppm. At this point, the $SO_2$ increased once again to a maximum of about 4 ppm. Then, after about 12 hr, the $SO_2$ decreased once again. Evolution of $SO_2$ was complete by 26 hr. The data is replotted in figure 9 for the total S evolved with time. For this curve, $SO_2$-$SO_3$-$O_2$ equilibrium was assumed and the total moles of S evolved were normalized by relating this total S to the number of moles of S that was present in the initial $Na_2SO_4$ coating.

## Calculated $SiO_2$ Formation During Hot Corrosion

Two simultaneous oxidation reactions are producing $SiO_2$ (or $SiO_2$-$Na_2O$ products) from $Si_3N_4$. For example, $Na_2SO_4$ reacts with $Si_3N_4$ to produce $Na_2SiO_3$ with an accompanying weight loss:

$$3Na_2SO_4(\ell) + Si_3N_4(s) + 3/2O_2(g) \rightarrow 3Na_2SiO_3(s) + 3SO_2(g) + 2N_2(g) \qquad (1)$$

$$SO_2(g) + 1/2O_2(g) \rightleftarrows SO_3(g) \qquad (2)$$

The extent of reaction 1 can be estimated from $SO_2$ evolution data (fig. 9).

At the same time, $O_2$ reacts with $Si_3N_4$ (without $Na_2SO_4$) to produce $SiO_2$ with an accompanying weight gain:

$$Si_3N_4(s) + 3O_2(g) \rightarrow 3SiO_2(s) + 2N_2(g) \qquad (3)$$

The extent of this reaction can be estimated by comparing the total weight changes as measured by the electrobalance with the $SO_2$ data. By way of illustration, figure 9 indicates that about 0.0328 mmol of total S were evolved after 10 hr from a sample containing an initial $Na_2SO_4$ coating of about 12 mg. Referring to equation (1), this represents a weight loss of about 2.19 mg. But, only about 1.79 mg were lost, as measured by the electrobalance, indicating that about 0.40 mg were gained by equation (3) (or 1.80 mg of $SiO_2$). Consequently, a total of about 3.77 mg of $SiO_2$ was produced during the hot corrosion process after 10 hr. The results will be discussed in more detail later in the discussion section.

## Film Morphology

A SEM photograph (fig. 10(a)) shows that the $Si_3N_4$ starting material has some pores (up to 1 $\mu$) even though the density of the hot-pressed material was about 98 percent. The extent of interconnection between pores is unknown but seems to be relatively small. EDAX measurements for this material are shown in figures 10(b) and (c) indicating that Si (at 1.8 keV) was the primary constituent with W (8.4 keV) and Y (14.8 keV) as the principal impurities. EDAX mapping suggested that Y and W were equally dispersed throughout the sample and not clustered in clumps.

For comparison, a SEM (fig. 10(d)) shows the outer surface of a $Si_3N_4$ sample (with no $Na_2SO_4$ coating) which was oxidized at 1000 °C for 75 hr. The outer surface after oxidation has a glassy appearance and contains considerable gas bubble holes.

Optical photographs of the outer surfaces of $Si_3N_4$ before and after hot corrosion are shown in figure 11. The hot corrosion process is clearly reflected in these outer surfaces. Up to about 3 hr, a smooth, glassy film is formed with some slight cracking and spalling near the bottom of the sample. This is illustrated in a SEM photograph (fig. 12(a)) for a sample that was hot corroded for 2 hr. The gas bubble holes are clearly visible. EDAX measurements (figs. 12(b) and (c)) show that Si is the principal constituent here along with a trace of Y. No appreciable Si, W, or Na were found in this phase. Any $Na_2SO_4$, remaining unreacted lies, presumably, just below this glassy phase. This is illustrated in figure 12(d), for a SEM photograph focused on one of the cracks near the bottom of the sample, where two separate phases of glassy Si and $Na_2SO_4$ were observed. EDAX mapping of this region showed that the $Na_2SO_4$ and the glassy Si were relatively immiscible in each other.

This glassy phase was unstable to long time air exposure. For example, exposure for 4 to 5 months leads to crystallization of the surface to form crystals containing primarily Si (i.e., $SiO_2$).

For the interval of about 4 to 15 hr, $Na_2SO_4$ was found at the outer surface in increasing amounts, particularly near the bottom of the sample (fig. 11). Small blisters are starting to form at the surface particularly after about 10 to 12 hr. And, gas evolution is now more rapid. Both are illustrated in figure 13 for a sample that was hot corroded for 9 hr. For example, the SEM given in figure 13(a) is focused on a spot in the glassy region where the gas evolution had been particularly vigorous. EDAX measurements for this region (figs. 13(b) to (d)) showed that this glassy phase contained primarily Si, Na, and a trace of Y but little or no S or W. As an approximation, the calibration factors for the peak heights for S and Si is assumed to be equal to 1. By referring to an EDAX for $Na_2SO_4$, a calibration factor of about 20 is calculated for the Na peak relative to Si. Using these factors, the overall approximate composition of the glassy phase (fig. 13(a)) was 65 and 35 wt % $SiO_2$ and $Na_2O$, respectively (i.e., about $Na_2Si_2O_5$).

A cross section of a sample that was hot corroded for a similar time of about 10 hr is given in figure 14. These SEM photographs clearly show the formation of blisters near the bottom of the sample. Presumably, these blisters are formed by puffing of the glassy film by the more rapid gas evolution.

EDAX measurements of the region in figure 14(c) suggests that the overall composition of the film is about 65 wt % $SiO_2$.

Referring once again to figure 11, blister formation at the outer surface is even more rapid and extensive particularly for times greater than about 20 hr. By this time, most of the $Na_2SO_4$ has decomposed. This formation of larger blisters is illustrated in figure 15(a) for a surface SEM photograph of a sample that was hot corroded for 23 hr at 1000 °C. Extensive gas evolution has occurred. This is illustrated even more clearly in figure 15(b) for a cross-section SEM photograph of the same sample.

## Chemical Analyses

Most of the sulfate was $H_2O$ soluble and found in the $H_2O$ leech liquors. For samples that were hot corroded for greater than 10 hr, a small quantity of sulfate was also found in the acidic HF liquors. This HF treatment decomposes the $H_2O$ insoluble phase containing Si (i.e., $SiO_2$) thereby freeing any trapped sulfate. The sulfate in the other two leech liquors was negligible. The total sulfate (remaining unreacted) was then determined by adding the quantities in each leech liquor. The results are plotted in figure 16 after correcting for the relatively minor $Na_2SO_4$ evaporation losses. For this plot, the results were normalized by relating them to the quantity of $Na_2SO_4$ in the original coating.

The total quantity of W in the surface film produced by the hot corrosion process was relatively small compared to the quantity of $Na_2SO_4$ decomposed. For example, only about 1.3 mg of W was obtained after 25 hr which is less that 10 mol percent of the $Na_2SO_4$ decomposed.

The total Y in the surface film was also relatively small being about 2.4 mg after 25 hr. Almost all of the Y was found in the acidic HF leech liquor suggesting that neither $Y_2(SO_4)_3$ nor $Y_2O_3$ were present in any significant quantities. Presumably, the Y was present as a Y silicate requiring HF to decompose the Si containing phase.

## DISCUSSION

Hot-pressed $Si_3N_4$ (without a $Na_2SO_4$ coating) was oxidized at 1000 °C under an atmosphere of flowing $O_2$ (at 8.3 $cm^3$ $sec^{-1}$). The primary oxidation reaction is as follows:

$$Si_3N_4(s) + 3O_2(g) \rightarrow 3SiO_2(s) + 2N_2(g) \qquad (4)$$

A parabolic weight gain rate constant of about $2 \times 10^{-12}$ $g^2$ $cm^{-4}$ $sec^{-1}$ was calculated from the continuous weight measurements.

This value is larger than a value of about $10^{-14}$ $g^2$ $cm^{-4}$ $sec^{-1}$ which was estimated from data presented by Cubicciotti for the oxidation of a similar type of hot-pressed $Si_3N_4$ which also contained $Y_2O_3$ as a dopant and W as a major impurity. Considering that a rather lengthy extrapolation of Cubicciotti's data (taken at higher temperatures) was required and that there were some differences in the impurity concentrations, the two values are in fair agreement. For example, the samples used in the present investigation contained about 3.1 wt % W

while Cubicciotti's samples contained a smaller value of about 2.1 percent W. The larger W content may have led to the faster oxidation rate.

It is assumed, therefore, that the oxidation of $Si_3N_4$ (without $Na_2SO_4$) used in the present investigation is diffusional controlled in a manner similar to that proposed by Cubicciotti. This process involved, essentially, diffusion of an impurity from within the $Si_3N_4$ sample (i.e., at the grain boundaries) to the surface where they can form small quantities of a silicate melt. Transport of $O_2$ and $N_2$ through this film is presumed to proceed more rapidly than through a solid, impervious $SiO_2$ film.

Continuous weight measurements, using a sensitive electrobalance, is a useful laboratory method for investigating hot corrosion of superalloys (in the presence of $Na_2SO_4$) where the weight gains are relatively large particularly for catastrophic-type oxidation. But depending solely upon weight measurements for investigating hot corrosion processes of $Si_3N_4$ may be misleading. This may be even more obvious if the weight measurements are not obtained continuously. First, the weight changes obtained during the hot corrosion of $Si_3N_4$ are relatively small. Second, unlike that observed for superalloys, the $Si_3N_4$ loses weight initially and then regains most of this weight loss. For example, for a sample containing a $Na_2SO_4$ coating of about 4.5 mg $cm^{-2}$, the sample after 25 hr now weighs essentially the same as it did initially at the start of the reaction. This weight loss and gain are due to two competing reactions: weight loss by a $Na_2SO_4$ reaction involving $SO_2$ evolution; and weight gain by a reaction involving $Si_3N_4$ oxidation.

Even though these weight changes were relatively small, the hot corrosion oxidation of $Si_3N_4$ was actually fairly large as suggested by the fact that all of the $Na_2SO_4$ had decomposed by 25 hr. And, the extent of the $Si_3N_4$ oxidation to produce $SiO_2$ was much greater in the case of hot corrosion than for oxidation in the absence of $Na_2SO_4$. For example, only about 2 mg of $SiO_2$ are produced by the oxidation process (without $Na_2SO_4$) after 25 hr while about 30 mg of $SiO_2$ (as $SiO_2 \cdot Na_2O$ products) were produced during the hot corrosion of $Si_3N_4$ (4.5 mg $cm^{-2}$ $Na_2SO_4$ coating). Therefore, weight measurement techniques with certain modifications are still useful for investigating hot corrosion of $Si_3N_4$. For the more effective utilization of this technique, however, the weight measurements should be made continuously and in conjunction with other techniques such as monitoring $SO_2$ evolution, observing film morphologies, and obtaining chemical analyses.

These multiple techniques, mentioned above, were used in the present hot corrosion study. Beyond 35 hr, the evaporation losses were larger than the corresponding weight gains from $Si_3N_4$ oxidation. For the period of about 25 to 35 hr, where all of the $Na_2SO_4$ has decomposed, the corrosion process is, presumably, similar to that process of oxidation of $Si_3N_4$ without $Na_2SO_4$ (eq. (3)) with a similar parabolic rate constant (i.e., $1 \times 10^{-12}$ $g^2$ $cm^{-4}$ $sec^{-1}$).

The hot corrosion period between 0 and 25 hr is of greater interest. In general, for the period between 0 hr and about 12 hr, the following were observed: the sample lost weight; $SO_2$ evolved at increasing concentrations until it reached a maximum of about 4 ppm; a glassy film containing Si was formed at the surface along with a relatively immiscible $Na_2SO_4$ phase; and $Na_2SO_4$ was decomposed continuously. Then, for the period of about 12 to 25 hr, the following were observed: the sample regained most of the weight that it

had lost initially; $SO_2$ evolution slowed and was completed by 25 hr; blister formation increased; and all of the $Na_2SO_4$ had been decomposed by 25 hr.

As mentioned previously, the hot corrosion process involves two simultaneous oxidation reactions (eqs. (1) to (3)). The total milligram of $SiO_2$, produced during the hot corrosion reactions at 1000 °C, were calculated and are shown in figure 17. In this figure, the logs of the milligram of $SiO_2$ are plotted against time. For comparison, the logs of the activities of $SiO_2$ at various $SiO_2$ mole fractions in the binary $Na_2O$-$SiO_2$ system are also plotted as a dashed line in figure 17. These $SiO_2$ activities were calculated from activity coefficient values presented by Charles for $SiO_2$ mole fractions between 0.50 and 0.75 (ref. 15). As seen in figure 17, these $SiO_2$ activities also follows, essentially, a log relationship with the $SiO_2$ mole fraction. A comparison of the two curves in figure 17 suggests that the rate of formation of $SiO_2$ during the hot corrosion process is related to the $SiO_2$ activities in the $Na_2O$-$SiO_2$ films for the entire time interval that $Na_2SO_4$ is present (i.e., to about 25 hr).

The $Na_2O \cdot SiO_2$ phase diagram, reproduced in figure 18, shows that the system is complex with liquid phases being present at 1000 °C (ref. 16). For example, between 57 and 76 wt % $SiO_2$ (58 and 78 mol percent), the phase at 1000 °C is completely molten. Diffusional processes (e.g., $O_2$) through these molten films should be more rapid than through thick, solid, impervious $SiO_2$ films.

A relatively simple process is proposed for the hot corrosion of the hot-pressed $Si_3N_4$ at 1000 °C. This is illustrated in figure 19. It is proposed that the rate of reaction is related to the activity of the $SiO_2$ in the $Na_2O$-$SiO_2$ film produced at the surface. Any $SiO_2$ that forms during the oxidation by the hot corrosion process can move into the $Na_2O \cdot XSiO_2$ phase where the $SiO_2$ activity is much less. Diffusion of this species through this $Na_2O \cdot XSiO_2$ phase, particularly for the completely molten range of 57 to 76 wt % $SiO_2$, should be fairly rapid. Upon reaching the $Na_2SO_4$ interface, it can react there with $Na_2SO_4$ to evolve $SO_2$. The process would come to an end when the $Na_2O$-$SiO_2$ melt is saturated with $SiO_2$ e.g., when the $SiO_2$ content of the melt corresponds to the liquidus composition in the $SiO_2$ side of the $Na_2O$-$SiO_2$ phase diagram.

## CONCLUSIONS

Laboratory weight measurement techniques can be used to follow the hot corrosion of $Si_3N_4$ even though the weight changes are relatively small. But, for the most effective utilization of this technique, the weights should be measured continuously and in conjunction with other techniques such as $SO_2$ measurements, film morphology observations, and analyses.

Oxidation of hot-pressed $Si_3N_4$ (in the absence of $Na_2SO_4$) proceeds relatively slowly. It is proposed that it proceeds in a manner similar to that process proposed by Cubicciotti for a similar type of $Si_3N_4$. Even though the measured weight changes were small during the hot corrosion process, the actual oxidation attack of the $Si_3N_4$ was fairly extensive. For example, about 30 mg of $SiO_2$ were formed after 25 hr during the hot corrosion attack while oxidation without $Na_2SO_4$ produced only about 2 mg.

A simple mechanism has been proposed for the hot corrosion of $Si_3N_4$ which is related to the $SiO_2$ activity in the $Na_2O \cdot XSiO_2$ phase. Oxidation of the $Si_3N_4$ produces $SiO_2$ that moves quickly into the $Na_2O \cdot XSiO_2$ phase which have activities less than one. These $SiO_2$ species can move through this $Na_2O \cdot XSiO_2$ phase to the $Na_2SO_4$ interface where they can react with the $Na_2SO_4$ to evolve $SO_2$. The reaction stops when the melt is saturated with $SiO_2$ e.g., when the $SiO_2$ content of the melt corresponds to the liquidus composition in the $SiO_2$ rich side of the $Na_2O$-$SiO_2$ phase diagram.

## REFERENCES


1. Battelle: Engineering Property Data on Selected Ceramics Volume I, Nitrides, MCIC-HB-07-Vol. I, p. 5.3.0-1, March 1976.

2. Singhal, S.C.: Thermodynamics and Kinetics of Oxidation of Hot-Pressed Silicon Nitride, J. Mater. Sci., 11 (3) pp. 500-509 (1976).

3. Cubicciotti, D.; and Lau, K.H.: Kinetics of Oxidation of Hot-Pressed Silicon Nitride Containing Magnesia, J. Am. Ceram Soc., 61, pp. 512-517 (1978).

4. Cubicciotti, D.; and Lau, K.H.: Kinetics of Oxidation of Yttria Hot-Pressed Silicon Nitride, J. Electrochem Soc., 126 (10), pp. 1723-1728 (1979).

5. Stringer, J.: Hot Corrosion of High Temperature Alloys, in Properties of High Temperature Alloys, ed. by Z.A. Fouroulis and F.S. Pettit, The Electrochemical Society, Inc., Princeton, New Jersey, pp. 513-556.

6. Richerson, D.W.; and Yonushonis, T.M.: Environmental Effects on the Strength of Silicon-Nitride Materials, MCIC-78-36 Report 1978, p. 249 (1978).

7. Singhal, S.C.: Corrosion Behavior of Silicon Nitride and Silicon Carbide in Turbine Atmospheres, MCIC-73-19, pp. 245-250 (1973).

8. Tressler, R.E.; Meiser, M.D.; and Yonushonis, T.: Molten Salt Corrosion of SiC and $Si_3N_4$ Ceramics, J. Am. Ceram. Soc, 59 (5-6), pp. 278-279 (1976).

9. Jacobson, N.S.; and Smialek, J.L.: Hot Corrosion of Sintered $\alpha$-SiC, to be published.

10. Larsen, D.C.: Property Screening and Evaluation of Ceramic Turbine Engine Materials,, AFML-TR-79-4188, p. 35 (1979).

11. Schuon, S.: Effect of W and WC on the Oxidation Resistance of Yttria-Doped Silicon Nitride, NASA TM-81528 (1980).

12. Lange, F.F.; Singhal, S.C.; and Kuznik, R.C.: Phase Relations and Stability Studies in the $Si_3N_4$-$SiO_2$-$Y_2O_3$ Pseudo-Ternary System, Tech. Rept. No. 6, ONR N00014-74-C-0284, 1976.

13. Stearns, C.A.; Kohl, F.J.; Fryburg, G.C.; and Miller, R.A.: A High Pressure Modulated Molecular Beam Mass Spectrometric Sampling System, NASA TM-73720 (1977).

14. Lake, C.L.: Determination of Traces of Flourine or Sulfur by X-ray Analysis, Anal. Chim. Acta., 43 pp. 245-252 (1968).

15. Charles, R.J.: Activities in $Li_2O$-, $Na_2O$-, and $K_2O$-$SiO_2$ Solutions, J. Am. Ceram. Soc., 50 (12), pp. 631-641 (1967).

16. Kingery, W.D.; Bowen, H.K.; and Uhlmann, D.R.: Introduction to Ceramics, 2nd Ed., John Wiley and Sons, New York, p. 288, 1976.

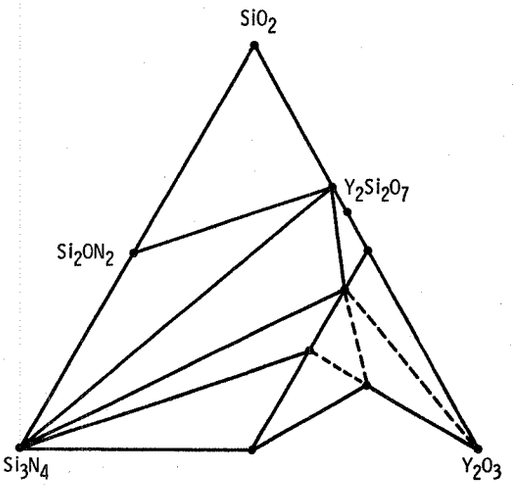


Figure 1. - Ternary phase diagram for the $Si_3N_4$-$SiO_2$-$Y_2O_3$ system.

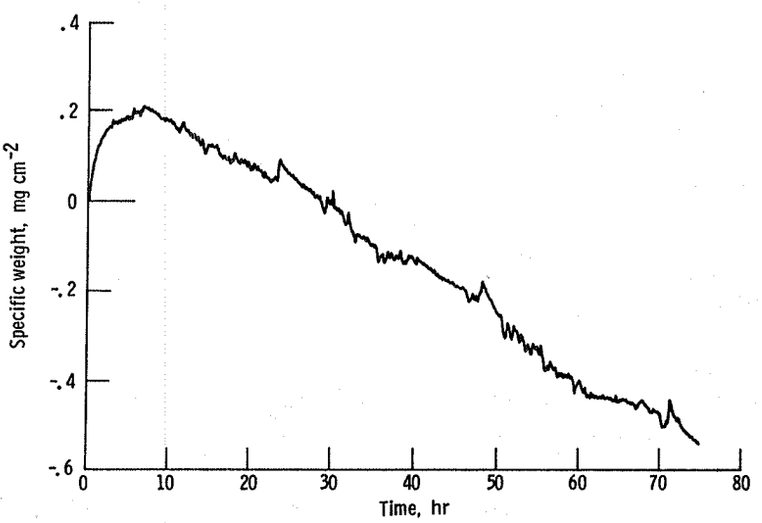


Figure 2. - Specific weight changes with time during $Si_3N_4$ oxidation at 1000 $^{o}$C. Flowing $O_2$ at 8.3 cm$^3$ sec$^{-1}$.

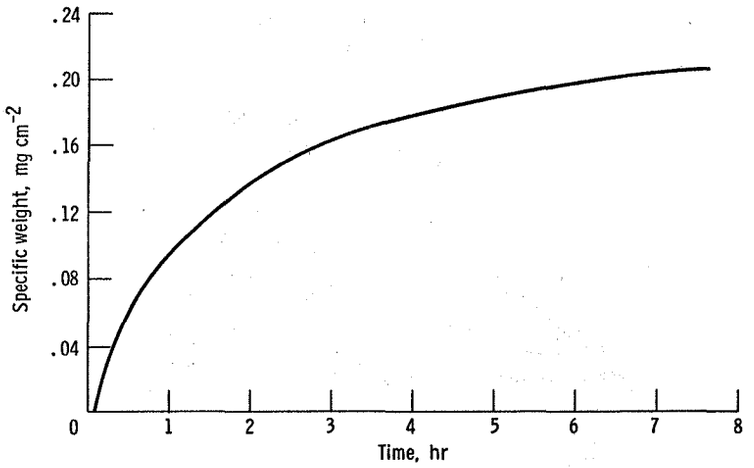


Figure 3. - Specific weight gains with time during $Si_3N_4$ oxidation at 1000 $^{o}$C. Flowing $O_2$ at 8.3 cm$^3$ sec$^{-1}$.

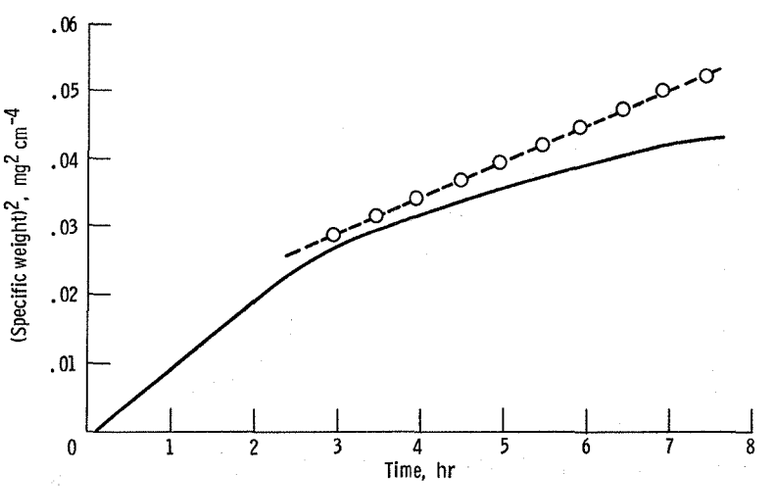


Figure 4. - Square of specific weight gain with time during $Si_3N_4$ oxidation at 1000 $^{o}$C. Flowing $O_2$ at 8.3 cm$^3$ sec$^{-1}$.

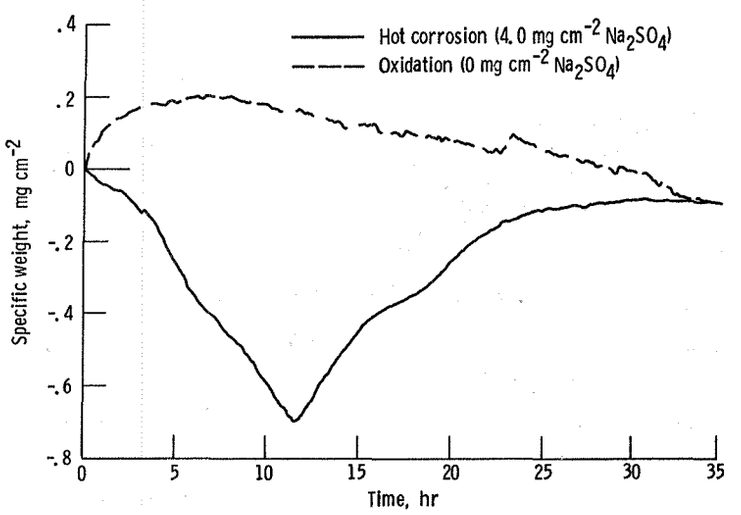


Figure 5. - Specific weight changes with time for hot corrosion and oxidation of $Si_3N_4$ at 1000 °C. Flowing $O_2$ at 8.3 cm$^3$ sec$^{-1}$.

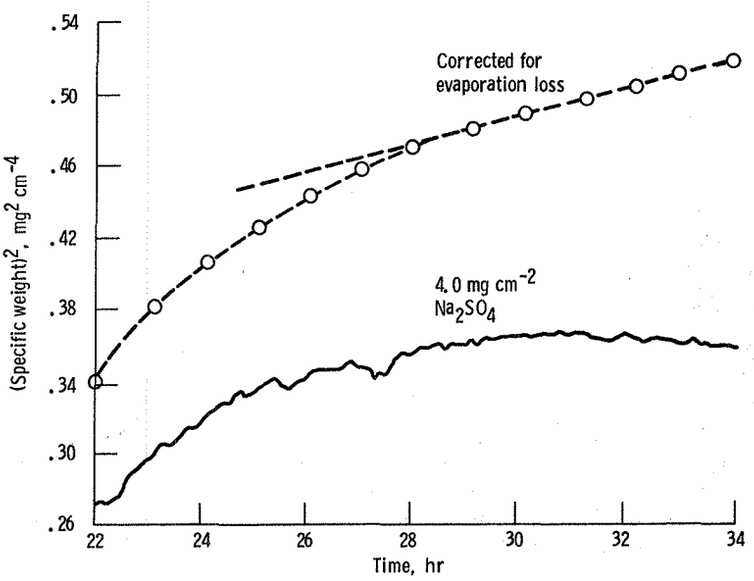


Figure 6. - Square of specific weight change with time during hot corrosion of $Si_3N_4$ at 1000 °C. Flowing $O_2$ at 8.3 cm$^3$ sec$^{-1}$.

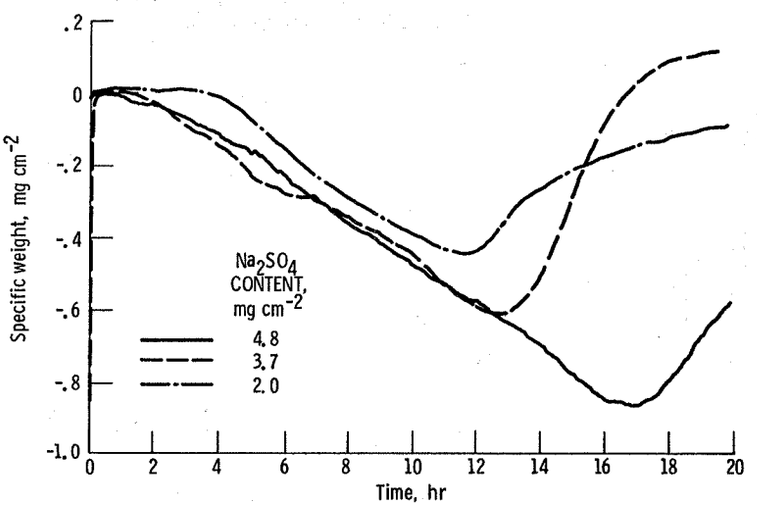


Figure 7. - Specific weight changes with time for hot corrosion at 1000 $^{o}$C of $Si_3N_4$ containing various $Na_2SO_4$ coating levels. Flowing $O_2$ at 8.3 cm$^3$ sec$^{-1}$.

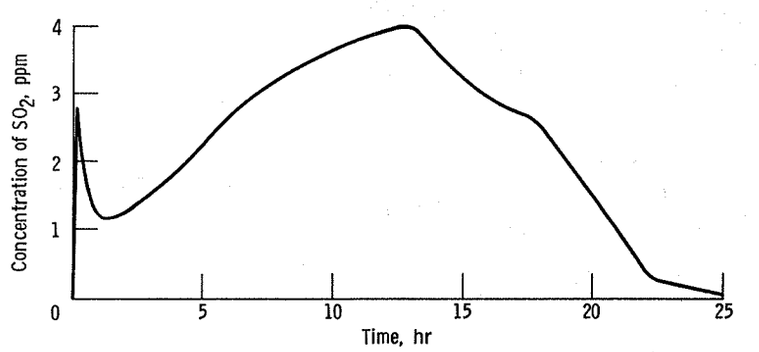


Figure 8. - Concentration of $SO_2$ with time during hot corrosion of $Si_3N_4$ at 1000 $^{o}$C. Flowing $O_2$ at 8.3 cm$^3$ sec$^{-1}$.

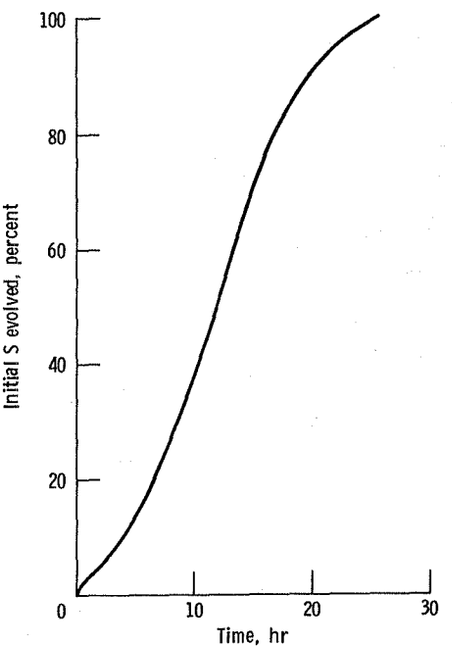


Figure 9. - Percent of initial S evolved, as $SO_2$ and $SO_3$, with time during hot corrosion at 1000°C of $Si_3N_4$ containing 4.5 mg $cm^{-2}$ $Na_2SO_4$. Flowing $O_2$ at 8.3 $cm^3$ $sec^{-1}$.

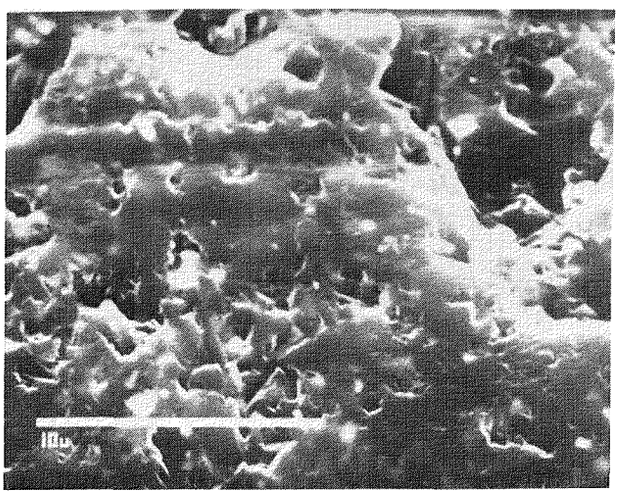

(a) SEM of unreacted $Si_3N_4$ (5000X).

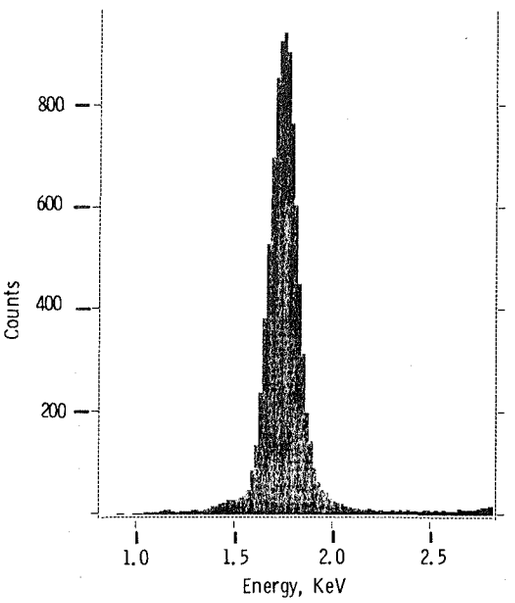


(b) EDAX of unreacted $Si_3N_4$ (Si) (5000X).

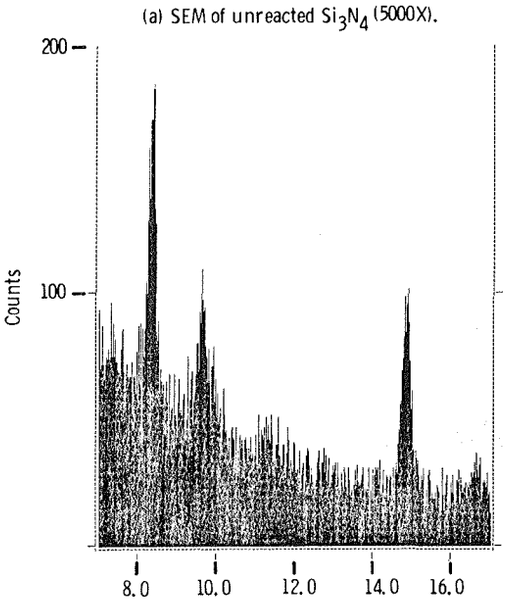


(c) EDAX of unreacted $Si_3N_4$ (W, Y) (5000X).

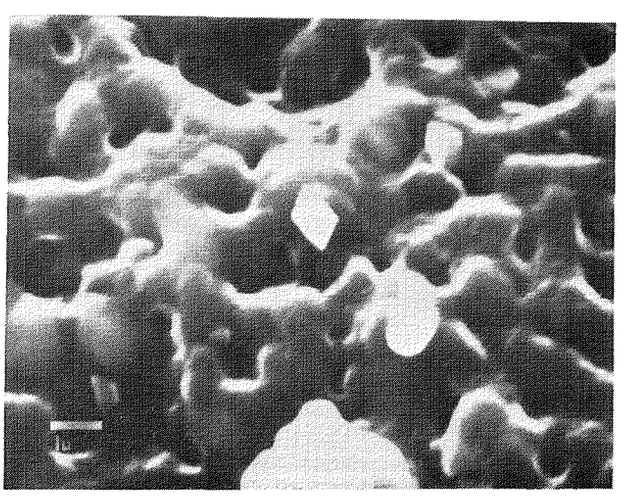

(d) SEM of oxidized $Si_3N_4$ (10,000X).

Figure 10. - SEM and EDAX of unreacted $Si_3N_4$ and SEM of $Si_3N_4$ (without $Na_2SO_4$) at 1000 $^0$C for 75 hours (8.3 $cm^3$ $sec^{-1}$ $O_2$).

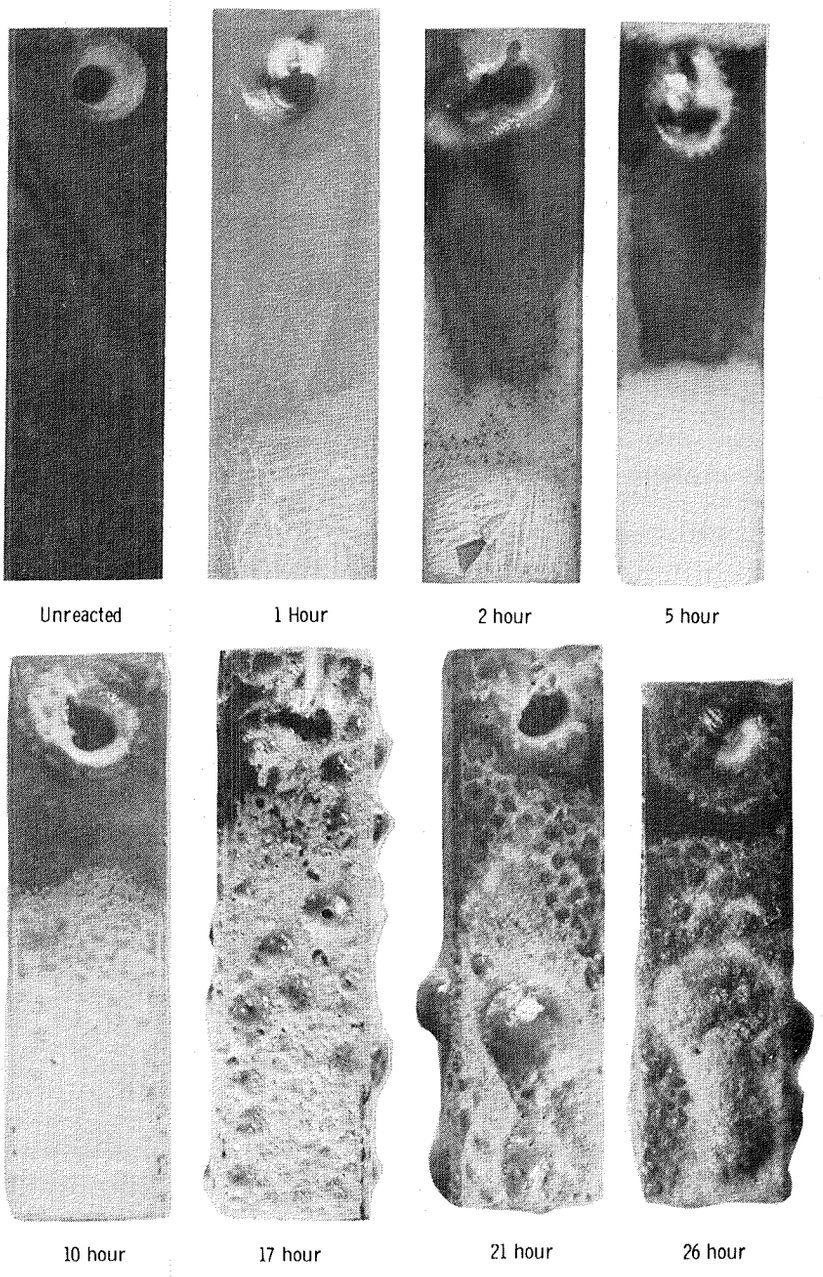


Figure 11. - Optical photographs (5X) of surfaces of unreacted $Si_3N_4$ and hot corroded $Si_3N_4$ containing about 4.5 mg $cm^{-2}$ $Na_2SO_4$ coating at 1000 $^{o}C$ (flowing $O_2$ of 8.3 $cm^3$ $sec^{-1}$).

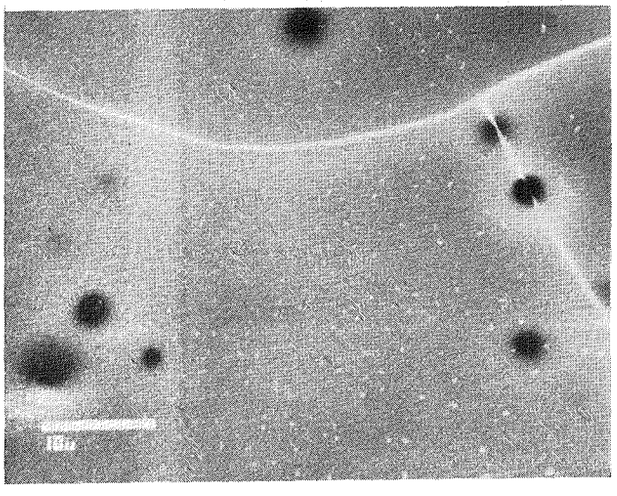

(a) SEM of glassy film (2000X).

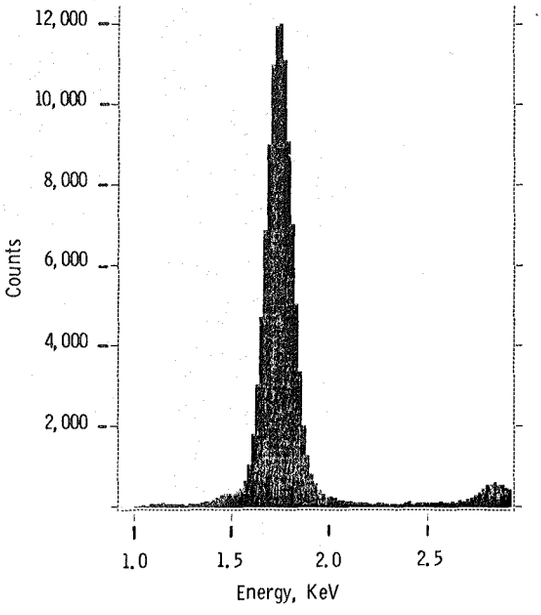


(b) EDAX of glassy film (Si) (2000X).

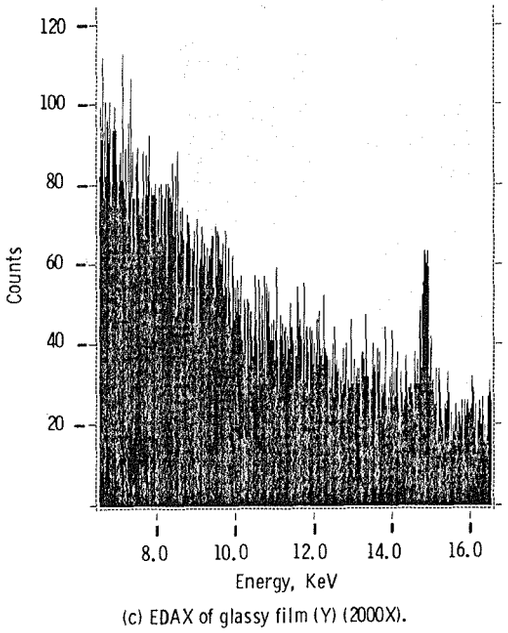


(c) EDAX of glassy film (Y) (2000X).

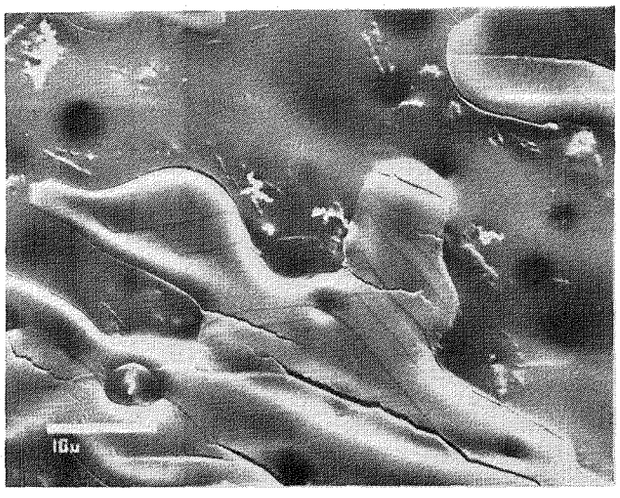

(d) SEM of spalled region (2000X).

Figure 12. - SEM and EDAX of $Si_3N_4$ containing about 4.5 mg $cm^{-2}$ $Na_2SO_4$ hot corroded at 1000 $^{o}C$ for 2 hours (flowing $O_2$ of 8.3 $cm^3$ $sec^{-1}$).

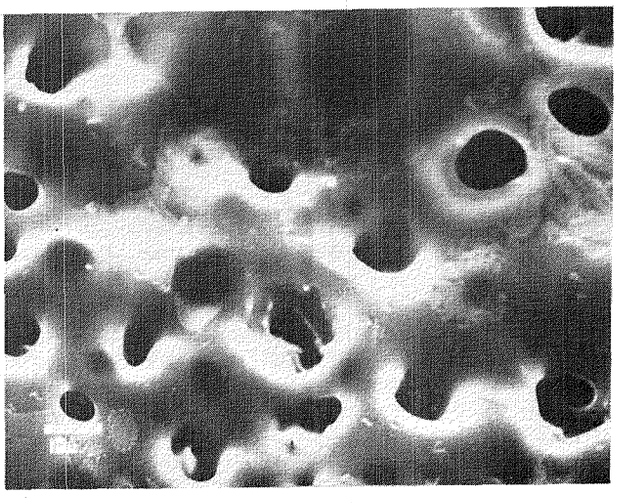

(a) SEM of glassy film (1000X).

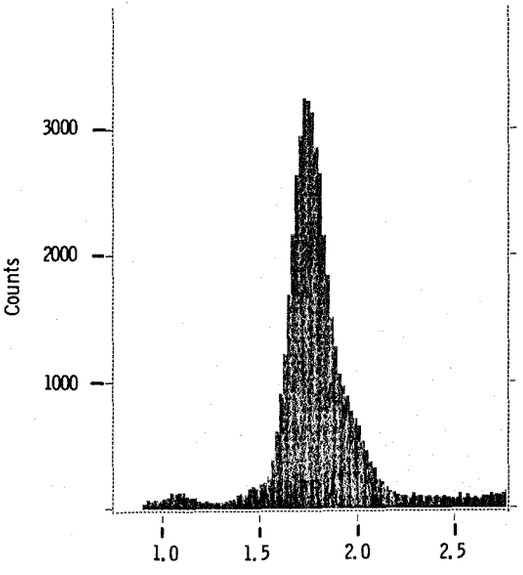


(b) EDAX of glassy film (Si) (2000X).

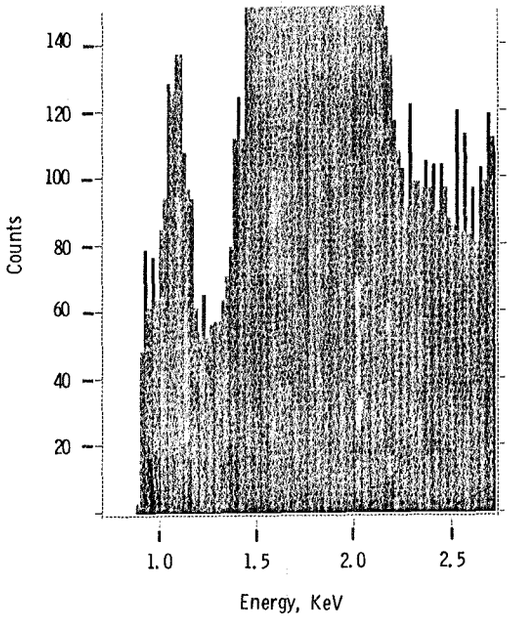


(c) EDAX of glassy film (Na) (2000X).

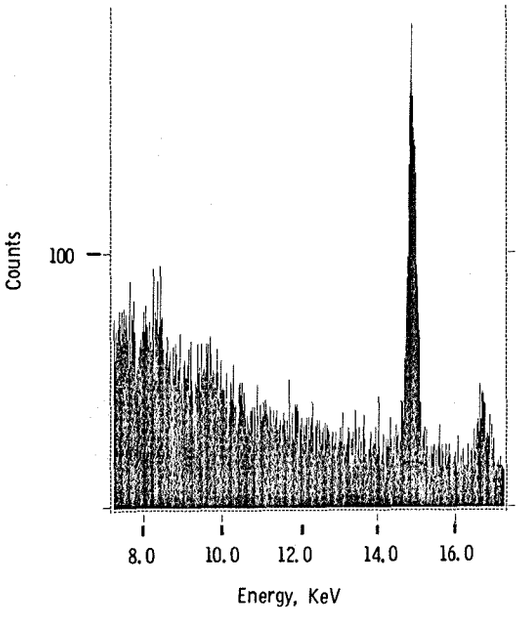


(d) EDAX of glassy film (Y) (2000X).

Figure 13. - SEM and EDAX of $Si_3N_4$ containing about 5.0 mg $cm^{-2}$ $Na_2SO_4$ hot corroded at 1000 $^0C$ for 9 hours (flowing $O_2$ at 8.3 $cm^3$ $sec^{-1}$).

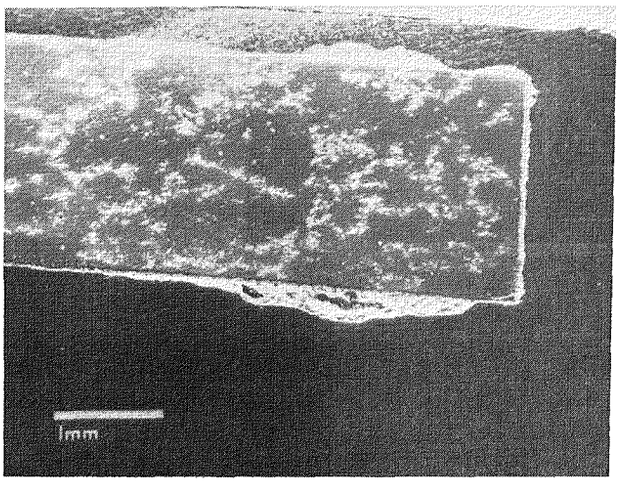


(a) Blister near sample bottom (20X).

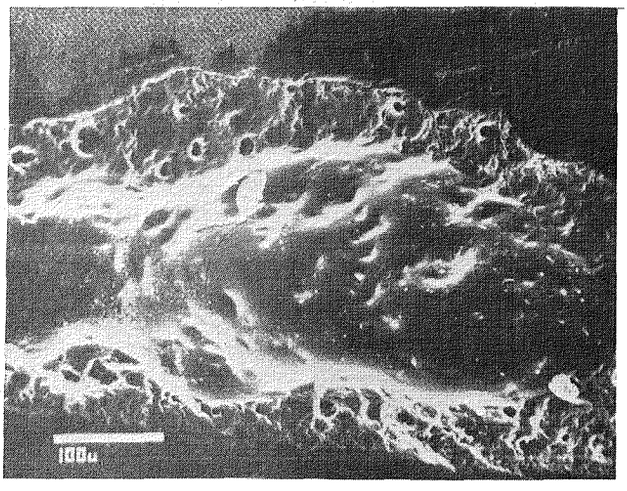


(b) Enlargement of upper blister in (a) (200X).

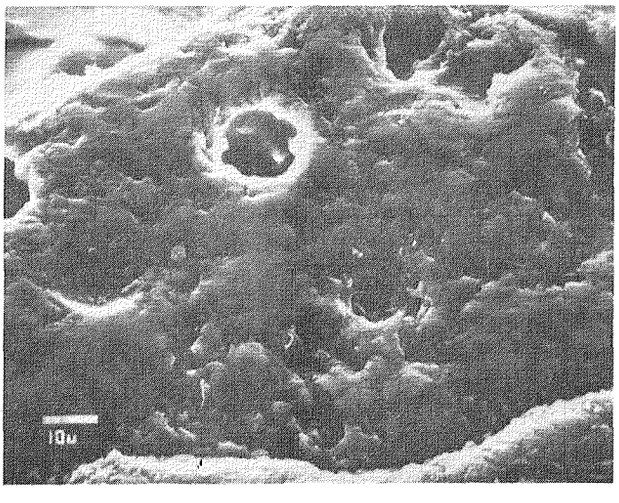


(c) Enlargement of top portion of blister in (b) (1000X).

Figure 14. - Cross section SEM of $Si_3N_4$ containing about 4.1 mg $cm^{-2}$ $Na_2SO_4$ hot corroded at 1000 $^0C$ for 10 hours (flowing $O_2$ at 8.3 $cm^3$ $sec^{-1}$).

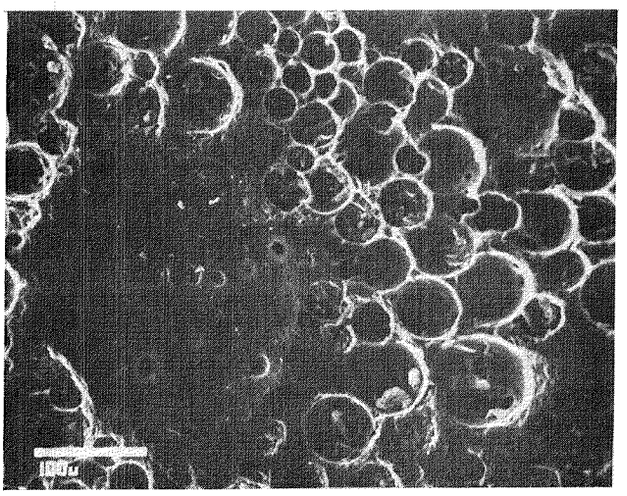

(a) SEM of blister surface (200X).

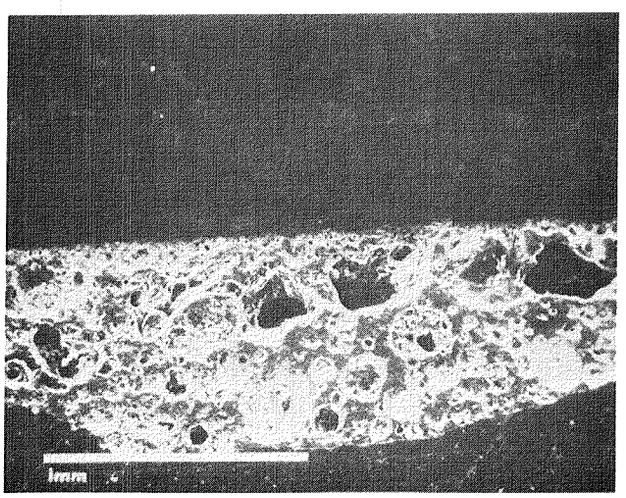

(b) SEM of blister cross section (50X).

Figure 15. - SEM of $Si_3N_4$ containing about 4.5 mg $cm^{-2}$ $Na_2SO_4$ hot corroded at 1000 $^{0}C$ for 23 hours (flowing $O_2$ at 8.3 $cm^3$ $sec^{-1}$).

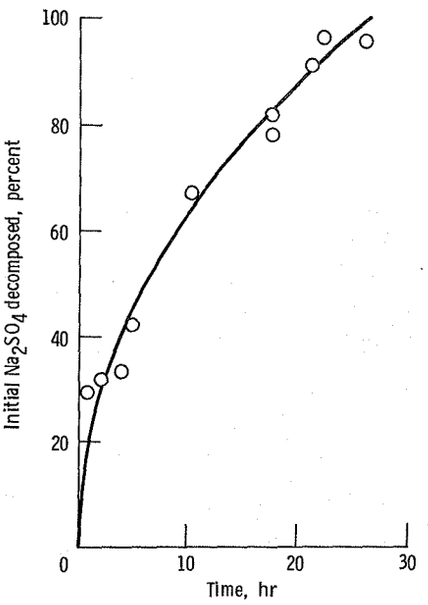


Figure 16. - Percent of initial $Na_2SO_4$ decomposed with time during hot corrosion of $Si_3N_4$ containing about 4.5 mg $cm^{-2}$ $Na_2SO_4$, at 1000 °C. Flowing $O_2$ at 8.3 $cm^3$ $sec^{-1}$.

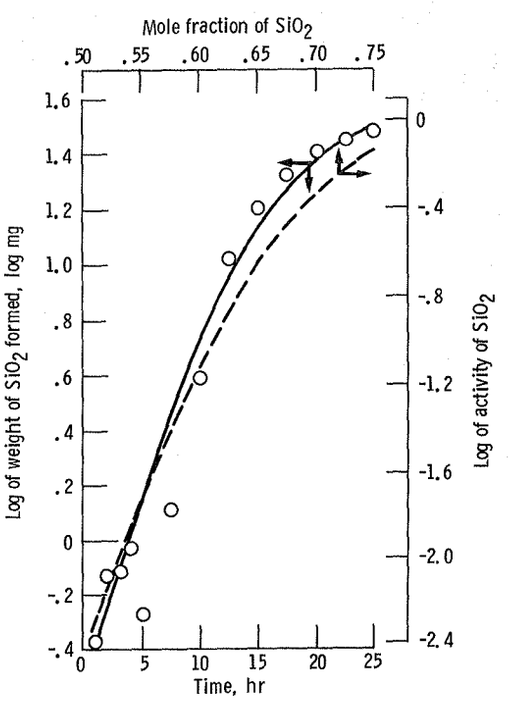


Figure 17. - Comparison of log of weight of $SiO_2$ formed with time during hot corrosion of $Si_3N_4$ (4.0 mg $cm^{-2}$ $Na_2SO_4$) at 1000 °C under flowing $O_2$ with log of $SiO_2$ activity versus its mole fraction.

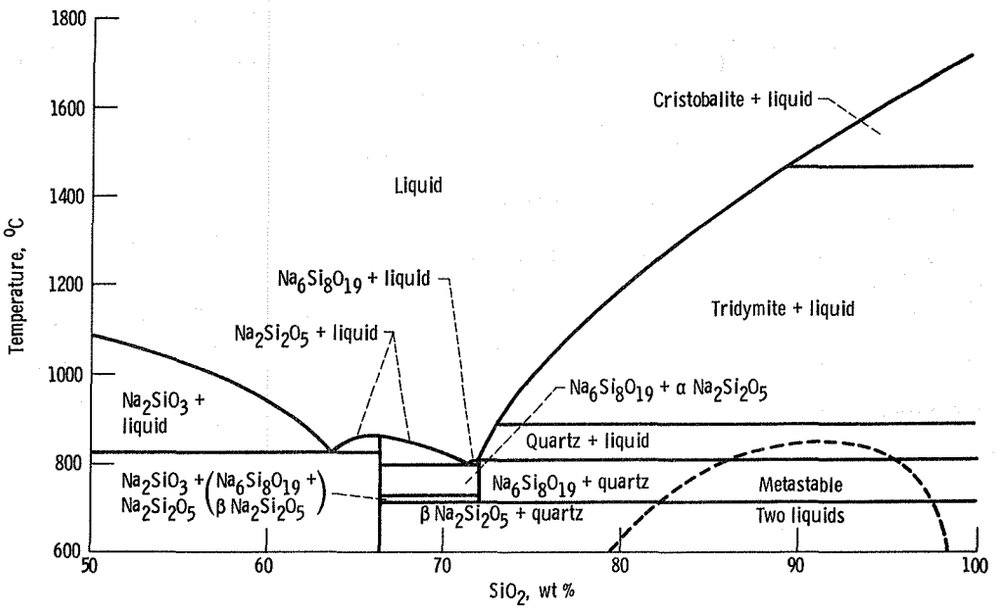


Figure 18. - The binary system $Na_2SiO_3$-$SiO_2$.

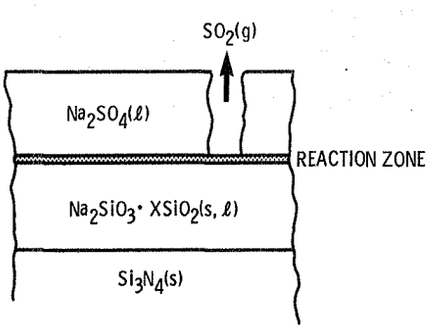


Figure 19. - A diagram representing the hot corrosion process of $Si_3N_4$ under flowing $O_2$.

| 1. Report No. | 2. Government Accession No. | 3. Recipient's Catalog No. |
|---|---|---|
| NASA TM-86977 | | |

| 4. Title and Subtitle | 5. Report Date |
|---|---|
| Oxidation and Hot Corrosion of Hot-Pressed $Si_3N_4$ at 1000 °C | April 1985 |
| | 6. Performing Organization Code<br>533-04-1C |

| 7. Author(s) | 8. Performing Organization Report No. |
|---|---|
| William L. Fielder | E-2419 |
| | 10. Work Unit No. |

| 9. Performing Organization Name and Address | 11. Contract or Grant No. |
|---|---|
| National Aeronautics and Space Administration<br>Lewis Research Center<br>Cleveland, Ohio 44135 | |
| | 13. Type of Report and Period Covered<br>Technical Memorandum |

| 12. Sponsoring Agency Name and Address | 14. Sponsoring Agency Code |
|---|---|
| National Aeronautics and Space Administration<br>Washington, D.C. 20546 | |

15. Supplementary Notes

16. Abstract

The oxidation and hot corrosion of a commercial, hot-pressed $Si_3N_4$ were investigated at 1000 °C under an atmosphere of flowing $O_2$. For the hot corrosion studies, thin films of $Na_2SO_4$ were airbrushed on the $Si_3N_4$ surface. The hot corrosion attack was monitored by the following techniques: continuous weight measurements; $SO_2$ evolution; film morphology; and chemical analyses. Even though the hot corrosion weight changes after 25 hr were relatively small, the formation of $SiO_2$ from oxidation of $Si_3N_4$ was an order of magnitude greater in the presence of molten $Na_2SO_4$ than for oxidation in the absence of $Na_2SO_4$. The formation of a protective $SiO_2$ phase at the $Si_3N_4$ surface is minimized by the fluxing action of the molten $Na_2SO_4$ thereby allowing the oxidation of the $Si_3N_4$ to proceed more rapidly. A simple process has been proposed to account for the hot corrosion process.

| 17. Key Words (Suggested by Author(s)) | 18. Distribution Statement |
|---|---|
| Hot corrosion<br>Silicon nitride<br>Ceramic | Unclassified - unlimited<br>STAR Category 27 |

| 19. Security Classif. (of this report) | 20. Security Classif. (of this page) | 21. No. of pages | 22. Price* |
|---|---|---|---|
| Unclassified | Unclassified | | |

*For sale by the National Technical Information Service, Springfield, Virginia 22161

End of Document